Supplementary Materials for "The benefits of ambitious short-term targets when decarbonising the European electricity and heating energy system"

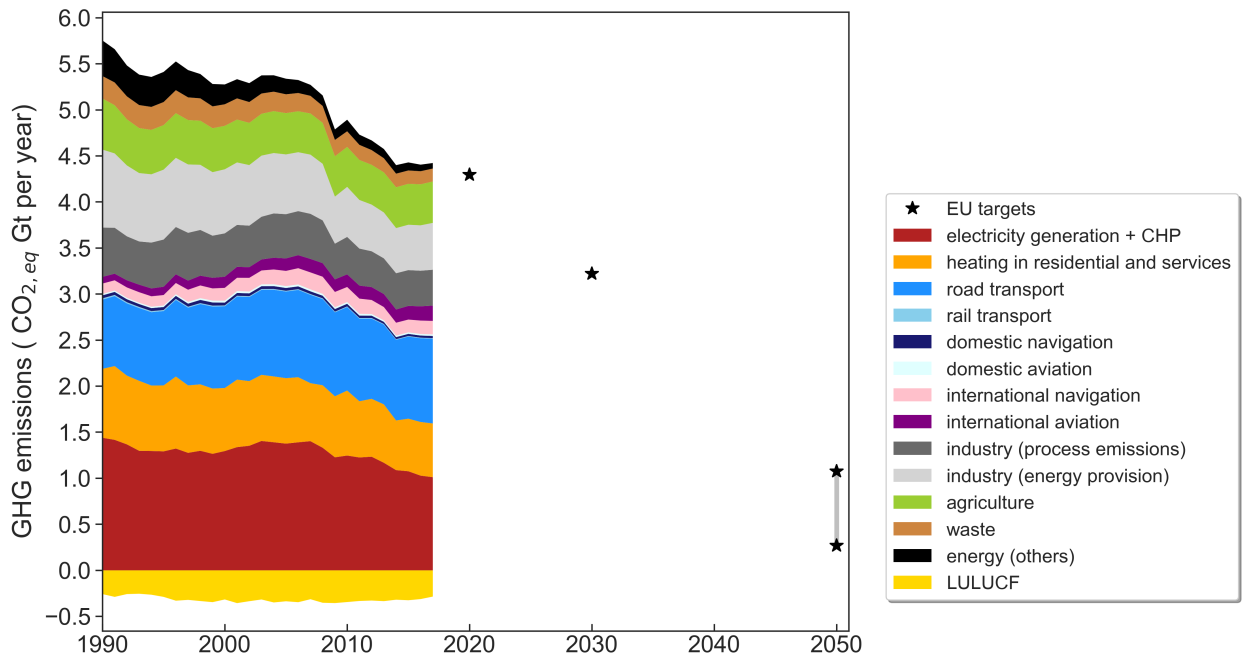## 1. Historical greenhouse gases emissions in the European Union

Figure 1: Sectoral distribution of historical emissions in the European Union [4]. The stars indicate committed EU reduction targets.

2. CO_2 restriction paths with equivalent budget

The carbon budget from now onwards for the generation of electricity and the supply of heating in residential and services sector in Europe accounts for 21 $GtCO_2$. It has been estimated based on a global carbon budget of 800 $GtCO_2$ to avoid temperature increments above 2°C relative to preindustrial period with a probability of greater than 66% [1, 2]. The global budget is assumed to be split among regions according to a constant per-capita ratio which translates into a 6% share for Europe [3]. Out of the total emissions in Europe, the ratio corresponding to electricity and heating is considered constant and equal to present values. In 2017, electricity generation and heating in the residential and services sector emitted 1.565 $GtCO_2$ with represents, 43.5% of European emissions [4].

The 21 $GtCO_2$ budget B can be spent following different transition paths. One option consists in assuming a linear CO_2 restriction path. Emissions will then reach zero in t_f

$$t_f = t_0 + \frac{2B}{e_0} \tag{1}$$

Where t_0=2020, and e_0 represents the carbon emissions from electricity and heating sector in 2020, which are assumed to be the same as in 2017.

Alternatively, emissions can be assumed to follow a path defined by one minus the cumulative distribution function (CDF_β) of a beta distribution in which $\beta_1 = \beta_2$.

$$e(t) = e_0(1 - CDF_\beta(t))$$
$$CDF_\beta(t) = \int_{-\infty}^{t} PDF(t)_\beta dt \tag{2}$$
$$PDF_\beta(t) = \frac{\Gamma(\beta_1 + \beta_2)}{\Gamma(\beta_1) + \Gamma(\beta_2)} t^{\beta_1 - 1}(1 - t)^{\beta_2 - 1}$$

where Γ is the gamma function. The cumulative emissions fulfil $\int_0^\infty e(t)dt = B$.

The third option considered is an exponential decay, following Raupach *et al.* [3]. In that case, emissions evolve as:

$$e(t) = e_0(1 + (r + m)t)e^{-mt} \tag{3}$$

where r is the initial linear growth rate, which is assumed r=0 here, and the decay parameter m is determined by imposing the integral of the path to be equal to the budget.

$$B = \int_0^\infty e_0(1 + (r + m)t)e^{-mt}dt$$
$$m = \frac{1 + \sqrt{1 + \frac{rB}{e_0}}}{\frac{B}{e_0}} \tag{4}$$

Although the exponential decay path approaches asymptotically to zero, we assumed here that $e(2050) = 0$. By doing that, the final point of the different transition paths is equivalent and all of them achieve net-zero emissions by 2050.

3. Historical evolution of heating supply in residential and services sector in European countries

4. Power plants in operation in Europe

5. Historical build rates for solar photovoltaics in European countries
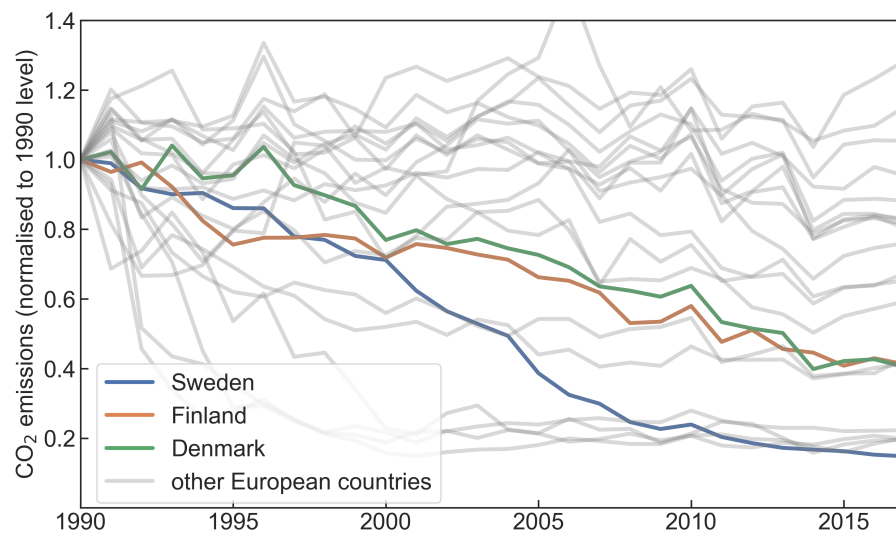
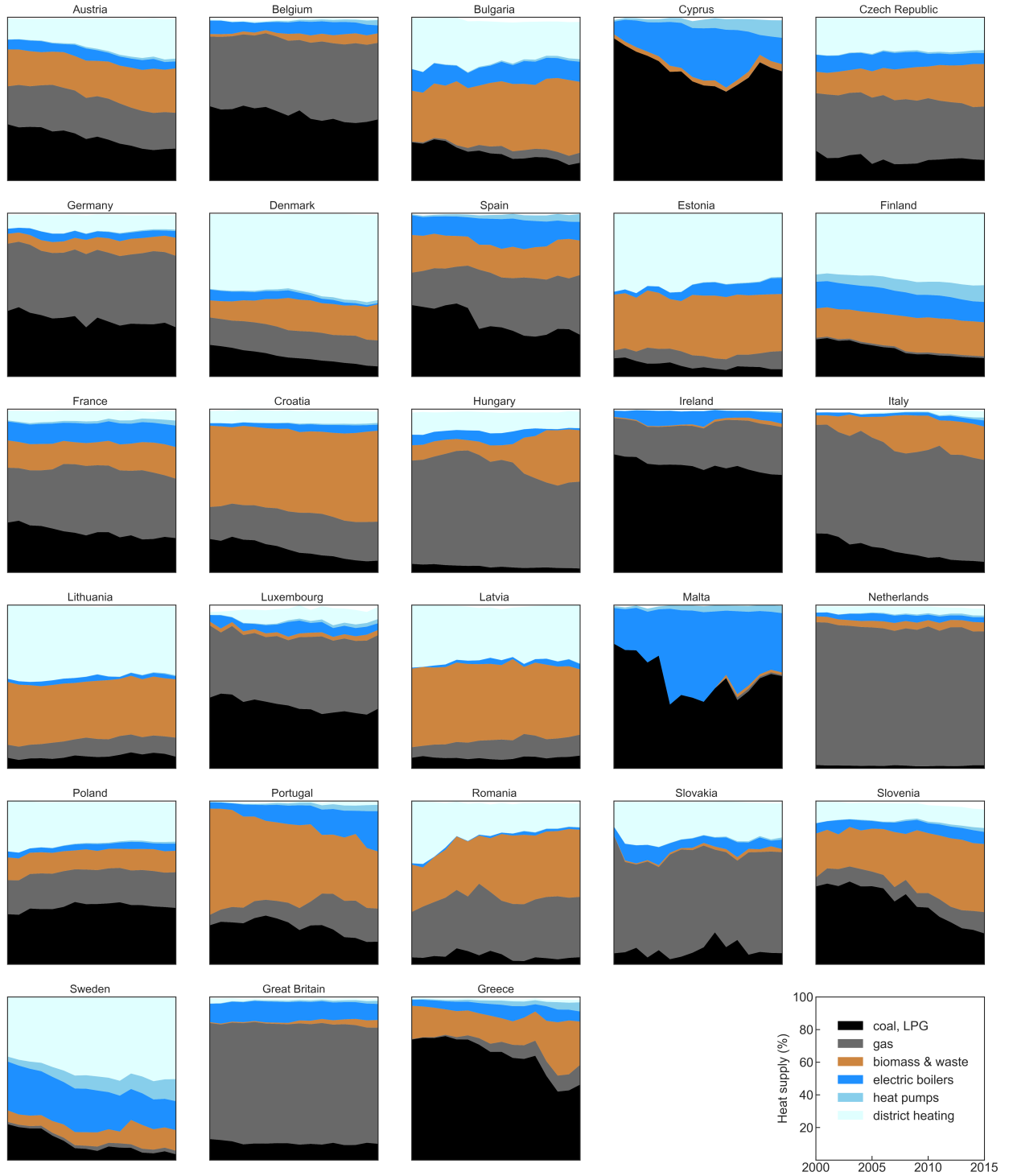Figure 2: Historical CO_2 emissions from heating in residential and services sector [4].

Figure 3: Historical share of technologies used to supply heating in residential and services sector [5].
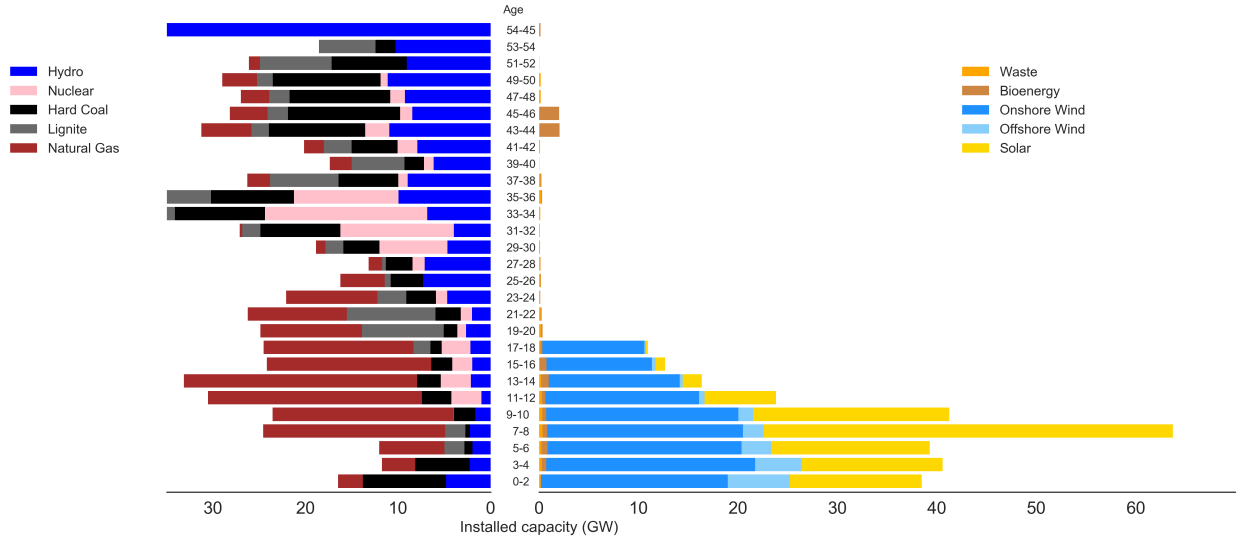
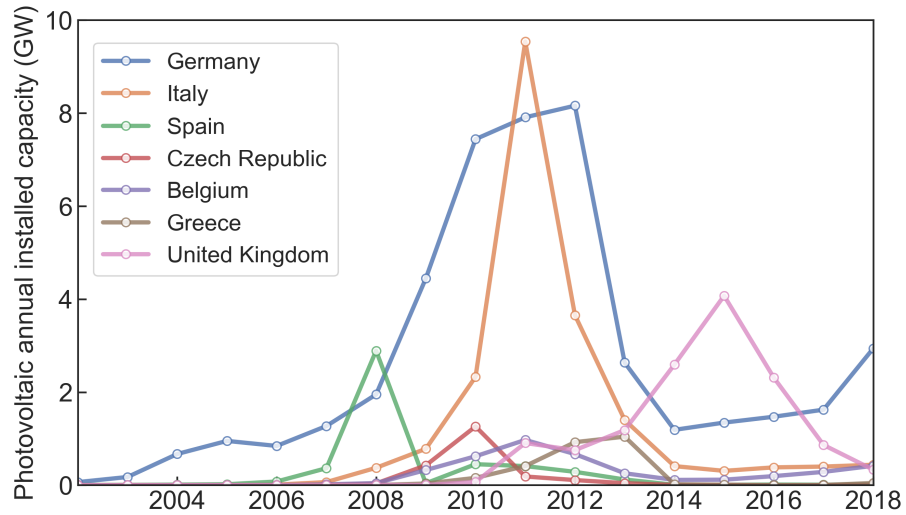Figure 4: Age distribution of European power plant in operation[6, 7]

Figure 5: Photovoltaic annual build rates for those European countries with a prominent peak [7]. The sharp increase and decrease in the installation rates were caused by country-specific successive changes in the regulatory frameworks.

6. Model description

In every time step, the optimisation objective, that is, the total annualised system cost is calculated as:

$$
\min_{\substack{G_{n,s}, E_{n,s}, \\ F_\ell, g_{n,s,t}}} \left[\sum_{n,s} c_{n,s} \cdot G_{n,s} + \sum_{n,s} \hat{c}_{n,s} \cdot E_{n,s} \right.
$$

$$
\left. + \sum_\ell c_\ell \cdot F_\ell + \sum_{n,s,t} o_{n,s,t} \cdot g_{n,s,t} \right] \tag{5}
$$

where $c_{n,s}$ are the fixed annualised costs for generator and storage power capacity $G_{n,s}$ of technology s in every bus n, $\hat{c}_{n,s}$ are the fixed annualised costs for storage energy capacity $E_{n,s}$, c_ℓ are the fixed annualised costs for bus connectors F_ℓ, and $o_{n,s,t}$ are the variable costs (which in some cases include CO_2 tax), for generation and storage dispatch $g_{n,s,t}$ in every hour t. Bus connectors ℓ include transmission lines but also converters between the buses implemented in every country (see Figure **??**), for instance, heat pumps that connect the electricity and heating bus.

The optimisation of the system is subject to several constraints. First, hourly demand $d_{n,t}$ in every bus n must be supplied by generators in that bus or imported from other buses. $f_{\ell,t}$ represents the energy flow on the link l and $\alpha_{n,\ell,t}$ indicates both the direction and the efficiency of flow on the bus connectors. $\alpha_{n,\ell,t}$ can be time dependent such as in the case of heat pumps whose conversion efficiency depends on the ambient temperature.

$$
\sum_s g_{n,s,t} + \sum_\ell \alpha_{n,\ell,t} \cdot f_{\ell,t} = d_{n,t} \quad \leftrightarrow \quad \lambda_{n,t} \quad \forall n, t \tag{6}
$$

The Lagrange multiplier $\lambda_{n,t}$, also known as Karun-Kush-Tucker (KKT), associated with the demand constraint indicates the marginal price of the energy carrier in the bus n, *e.g.*, local marginal electricity price in the electricity bus.

Second, the maximum power flowing through the links is limited by their maximum physical capacity F_ℓ. For transmission links, $\underline{f}_{\ell,t} = -1$ and $\bar{f}_{\ell,t} = 1$, which allows both import and export between neighbouring countries. For a unidirectional converter *e.g.*, a heat resistor, $\underline{f}_{\ell,t} = 0$ and $\bar{f}_{\ell,t} = 1$ since a heat resistor can only convert electricity into heat.

$$
\underline{f}_{\ell,t} \cdot F_\ell \leq f_{\ell,t} \leq \bar{f}_{\ell,t} \cdot F_\ell \qquad \forall \ell, t . \tag{7}
$$

For interconnecting transmission lines, the lengths l_ℓ are set by the distance between the geographical mid-points of each country, so that some of the transmission within each country is also reflected in the optimisation. A factor of 25% is added to the line lengths to account for the fact that transmission lines cannot be placed as the crow flies due to land use restriction. For the transmission lines capacities F_ℓ, a safety margin of 33% of the installed capacity is used to satisfy n-1 requirements [8]. Linear optimal power flow is applied using Kirchhoff's formulation [9].

Third, for every hour the maximum capacity that can provide a generator or storage is bounded by the product between installed capacity $G_{n,s}$ and availabilities $\underline{g}_{n,s,t}$, $\bar{g}_{n,s,t}$. For instance, for solar generators $\underline{g}_{n,s,t}$ is zero and $\bar{g}_{n,s,t}$ refers to the capacity factor at time t

$$
\underline{g}_{n,s,t} \cdot G_{n,s} \leq g_{n,s,t} \leq \bar{g}_{n,s,t} \cdot G_{n,s} \qquad \forall n, s, t . \tag{8}
$$

The maximum power capacity for generators is limited by potentials $\bar{G}_{n,s}$ that are estimated taking into account physical and environmental constraints:

$$0 \leq G_{n,s} \leq \bar{G}_{n,s} \qquad \forall\, n, s \;. \tag{9}$$

The storage technologies have a charging efficiency η_{in} and rate $g_{n,s,t}^{+}$, a discharging efficiency η_{out} and rate $g_{n,s,t}^{-}$, possible inflow $g_{n,s,t,\text{inflow}}$ and spillage $g_{n,s,t,\text{spillage}}$, and standing loss η_0. The state of charge $e_{n,s,t}$ of every storage has to be consistent with charging and discharging in every hour and is limited by the energy capacity of the storage $E_{n,s}$. It should be remarked that the storage energy capacity $E_{n,s}$ can be optimised independently of the storage power capacity $G_{n,s}$.

$$
\begin{aligned}
e_{n,s,t} &= \eta_0 \cdot e_{n,s,t-1} + \eta_{in}|g_{n,s,t}^{+}| - \eta_{out}^{-1}|g_{n,s,t}^{-}| \\
&\quad + g_{n,s,t,\text{inflow}} - g_{n,s,t,\text{spillage}} \;, \\
0 &\leq e_{n,s,t} \leq E_{n,s} \quad \forall\, n, s, t \;.
\end{aligned}
\tag{10}
$$

So far, equations (6) to (10) represent mainly technical constraints but additional constraints can be imposed to bound the solution.

The interconnecting transmission expansion can be limited by a global constraint

$$\sum_{\ell} l_{\ell} \cdot F_{\ell} \leq \text{CAP}_{LV} \qquad \leftrightarrow \quad \mu_{LV} \;, \tag{11}$$

where the sum of transmission capacities F_{ℓ} multiplied by the lengths l_{ℓ} is bounded by a transmission volume cap CAP_{LV}. In this case, the Lagrange/KKT multiplier μ_{LV} represents the shadow price of a marginal increase in transmission volume.

The maximum CO_2 allowed to be emitted by the system CAP_{CO2} can be imposed through the constraint

$$\sum_{n,s,t} \varepsilon_s \frac{g_{n,s,t}}{\eta_{n,s}} \leq \text{CAP}_{CO2} \quad \leftrightarrow \quad \mu_{CO2} \tag{12}$$

where ε_s represents the specific emissions in CO_2-tonne-per-MWh_{th} of the fuel s, $\eta_{n,s}$ the efficiency and $g_{n,s,t}$ the generators dispatch. In this case, the Lagrange/KKT multiplier represents the shadow price of CO_2, i.e., the additional price that should be added for every unit of CO_2 to achieve the CO_2 reduction target in an open market.

7. Sectors description and data

8. Cost assumptions

Figure 6: Cost evolution assumed for the different technologies.

9. References

[1] C. Figueres, H. J. Schellnhuber, G. Whiteman, J. Rockström, A. Hobley, S. Rahmstorf, Three years to safeguard our climate, Nature News 546 (7660) 593. doi:10.1038/546593a.
URL http://www.nature.com/news/three-years-to-safeguard-our-climate-1.22201
[2] G. Peters, How much carbon dioxide can we emit?
URL https://cicero.oslo.no/en/posts/climate/how-much-carbon-dioxide-can-we-emit

[3] M. R. Raupach, S. J. Davis, G. P. Peters, R. M. Andrew, J. G. Canadell, P. Ciais, P. Friedlingstein, F. Jotzo, D. P. Vuuren, C. L. Quéré, Sharing a quota on cumulative carbon emissions, Nature Climate Change 4 (10) (2014) 873–879. doi:10.1038/nclimate2384.
URL https://www.nature.com/articles/nclimate2384

[4] National emissions reported to the UNFCCC and to the EU Greenhouse Gas Monitoring Mechanism , EEA.
URL https://www.eea.europa.eu/data-and-maps/data/national-emissions-reported-to-the-unfccc-and-to-the-eu-greenhouse-gas-

[5] L. Mantzos, T. Wiesenthal, N. Matei, S. Tchung-Ming, M. Rzsai, H. P. Russ, A. Soria, JRC-IDEES: Integrated Database of the European Energy Sectordoi:10.2760/182725.
URL http://www.sciencedirect.com/science/article/pii/S0360544216310295

[6] powerplantmatching.
URL https://github.com/FRESNA/powerplantmatching

[7] Renewable Capacity Statistics 2019, IRENA.
URL https://www.irena.org/publications/2019/Mar/Renewable-Capacity-Statistics-2019

[8] T. Brown, P. Schierhorn, E. Tröster, T. Ackermann, Optimising the european transmission system for 77% renewable electricity by 2030 10 (1) 3–9. doi:10.1049/iet-rpg.2015.0135.

[9] J. Hörsch, H. Ronellenfitsch, D. Witthaut, T. Brown, Linear optimal power flow using cycle flows 158 (2019) 126–135. doi:10.1016/j.epsr.2017.12.034.
URL http://www.sciencedirect.com/science/article/pii/S0378779617305138

Table 1: Cost assumption per technology and year.

Technology[1]	2020	2025	2030	2035	2040	2045	2050	source
Battery inverter								
Battery storage								
Combined heat and power								
Coal power plant								
Direct air capture								
Electric boiler								
Electrolysis								
Fuel cell								
Gas boiler central								
Gas boiler individual								
Heat pump central								
Heat pump individual								
High voltage direct current line								
Hot water tank central								
Hot water tank individual								
Hydro reservoir								
Hydrogen storage								
Lignite power plant								
Methanation								
Nuclear								
Offshore wind								
Oil power plant								
Onshore wind								
Open cycle gas turbine								
Pumped hydro storage								
Run of river								
Solar PV rooftop								
Solar PV utility								

[1] Sorted by alphabet.

Table 2: Efficiency, lifetime and FOM cost per technology, include references.